

Implication of an Integrated Approach to the Determination of Water Saturation in a Carbonate Gas Reservoir Located in the Persian Gulf

Marzieh Neyzan Hosseini¹, Ezatallah Kazemzadeh^{2*}, Ehsan Sobhani³, and Bita Arbab⁴

¹ Department of Geophysics, College of Basic Science, Kermanshah Branch, Islamic Azad University, Kermanshah, Iran

² Department of Petroleum Engineering, Islamic Azad University, Science and Research Branch, Tehran, Iran

³ Department of Geophysics, College of Basic Science, Kermanshah Branch, Islamic Azad University, Kermanshah, Iran

⁴ Department of Petrophysics, Iranian Offshore Oil Company, Tehran, Iran

ABSTRACT

Water saturation determination is one of the most important tasks in reservoir studies to predict oil and gas in place needed to be calculated with more accuracy. The estimation of this important reservoir parameter is commonly determined by various well logs data and by applying some correlations that may not be so accurate in some real practical cases, especially for carbonate reservoirs. Since laboratory core analysis data have a high accuracy, in this study, it is attempted to use core and geological core description data to present an improved method to determine an optimized cementation factor (m) and a saturation exponent (n) in order to evaluate water saturation within carbonate reservoirs compared to default values ($m=2$, $n=2$, $a=1$) in a carbonate gas reservoir located in the Persian Gulf. Based on integrating core petrography and velocity deviation log (VDL), core samples were classified based on the type of porosity and geology description, and then by employing log-log plots of formation resistivity factor (FRF) versus porosity and formation resistivity index (FRI) versus water saturation, saturation parameters (m, n) were determined for each classification. Utilizing default and optimized values of saturation parameters, water saturation logs were obtained through different conductivity models by employing Multi min algorithm. Then, optimized water saturation was compared to core data. Error analysis showed that water saturation data resulted in optimized saturation parameters having a lower average error of 0.08 compared to the default ones with an average error of 0.14, and based on cumulative histogram, optimized water saturation data are in good agreement with the trend of core water saturation.

Keywords: Water Saturation, Saturation Parameters, Petrography, Velocity Deviation Log

INTRODUCTION

One of the key petrophysical parameters for evaluating reserve estimation is water saturation. In order to calculate the hydrocarbon reserve, one needs to know the water saturation amount. The improper calculation of water saturation leads

to great errors in reserve estimation. Traditional methods for obtaining water saturation were based on the assessment of core samples which were drilled using oil based mud. Nevertheless, due to the technical difficulties and costs, these methods could only measure saturation for few points.

*Corresponding author

Ezatallah Kazemzadeh

Email: kazemzadehe@ripi.ir

Tel: +98 21 4473 9761

Fax: +98 21 4473 9742

Article history

Received: May 21, 2016

Received in revised form: August 20, 2016

Accepted: August 22, 2016

Available online: Jun 20, 2017

In 1942, Archie proposed a sound physical and much easier method which relates water saturation to the formation porosity and resistivity. In a clean formation, Archie's equation is given by:

$$S_w^n = FRF \frac{R_w}{R_t} \quad (1)$$

where, S_w is water saturation, and n is an exponent of water saturation; R_w represents the formation brine resistivity, and R_t stands for the fluid resistivity of uninvaded zone (brine and hydrocarbon); FRF is the formation resistivity factor given by:

$$FRF = \frac{\alpha}{\phi^m} \quad (2)$$

where, α is tortuosity factor, and ϕ and m are porosity and an exponent depicting the cementation degree of a formation respectively.

Another useful representation of the Archie's equation is based on the formation resistivity index (FRI) defined as follows:

$$FRI = \frac{R_t}{R_o} = \frac{1}{S_w^n} \quad (3)$$

where, R_o is the resistivity of rock fully saturated with brine (formation water) [1].

There are a number of assumptions for Archie's equation, including (1) rock surface to be strongly water-wet and (2) pore system to be free of clay minerals. These assumptions are not always guaranteed, especially when one is dealing with carbonate rocks owing to complex pore geometry and a high degree of local heterogeneity.

Clay mineral in the rock matrix acts as an electrolyte conductor, so they introduce a new conduction path for ions similar to the formation water. Since 1950, the clay problem has been fully recognized and addressed. The clay models have been divided into two main groups [2]: (1) Models based on the clay volume fraction such as Hossin, Simandoux, Bardon & Pied, Worthington, and Indonesia model. The disadvantage of these models is that they do not take account of the composition of constituent clays [2-6].

(2) Models based on the ionic double-layer phenomenon such as Waxman & Smith and Dual-water [7, 8].

The second group models take account of the composition of constituent clays, but parameters such as cation exchange capacity (CEC) have directly been brought from core samples in laboratory, while for the first group clay volume fraction can indirectly be determined from well log data.

There have been efforts in the past for calculating water saturation exponent (n) from only well logs [9]. The water saturation exponent (n) has been reported to be equal to 2.0 for clean, consolidated, and water-wet sandstones and has been assumed equal to 2.0 in many petrophysical evaluation equations. In reality, however, n is not constant, but it varies as a function of different factors, including fluid distribution in pore spaces and rock wettability. The traditional method to determine n is plotting FRI versus water saturation on a logarithmic scale and calculating the slope of straight line fitting to the data points.

Many studies have noticed the proportionality of m , the cementation factor, to the formation porosity. Considering this, the number of correlations are established using porosity logs. However, in all of these works, the tortuosity of the pore network is neglected, and they concluded that the cementation factor depends on the pores geometry and the degree of their interconnectivity. Therefore, the variation of pore type is of significant importance with respect to m , and it is needed to group data to identify this variation. Uncertainty analysis has shown that among various parameters, the cementation factor has the highest impact. The common method to estimate m is the slope of the straight line fitting the formation resistivity factor versus porosity on a logarithmic scale. The best fit will achieve when the variation of the tortuosity is considered [10-16].

This study has been focused on the investigation of more accurate and optimum petrophysical parameters to calculate and determine water saturation profile by a suitable water saturation model for carbonate reservoirs of an offshore gas field in the Persian Gulf. Four wells have been drilled in this field and core analysis data are only available for one well, which is selected for our purpose.

EXPERIMENTAL PROCEDURES

Methodology

Geological core description and special core analysis data along with resistivity and porosity logs for one of the wells in the considered carbonate gas field were selected in order to determine water saturation. Figure 1 shows a part of petrography results; according to the petrography studies, carbonate reservoirs of the field mainly consist of limestone

and dolomite. At many depths, pore spaces have been filled with anhydrite cement. Interparticle, moldic, and inter crystalline are porosity types in reservoirs, and in some limited depths vuggy porosity exists.

In this study, 97 core samples have been used for the core analysis. FRF and FRI measurements have been performed for 32 core samples. Relative permeability and irreducible water saturation data have been measured for 64 core samples. Since core water saturation data were not available, irreducible water saturation data in the reservoir section above oil-water contact and transition zone were used to compare with the water saturation obtained from petrophysical modeling.

Table 1 shows FRF and porosity measurements at a confining pressure of 6200 psi corresponding to the reservoir pressure.

Plug No.	Depth (m)	Lithology (%)					Bioclast (%)							Facies code	Facies			
		Limestone (%)	Dolostone (%)	Anhydrite (%)	Sandstone (%)	Clay (%)	Matrix + Porosity (%)	Main Lithology	Fine skeletal debris	Large skeletal debris	Benthic forams	Planctonic forams	Peloid			ooid	Intraclast	oncolid
01H	3457.25	100	0	0	0	0	100	l									4	mudstone
01V	3457.4	0	100	0	0	0	100	d									4	dolomudstone
02H	3457.5	0	95	0	0	0	100	d									4	dolomudstone
03H	3457.98	0	90	0	0	0	100	d									4	dolomudstone
04H	3458.13	70	25	5	0	0	100	dl		20		5	30				8	skeletal ooid grainstone
05H	3458.62	75	20	5	0	0	100	dl		10			70				8	ooid grainstone
06H	3458.84	92	5	3	0	0	100	l		40			30	5			8	ooid skeletal grainstone
02V	3458.94	98	0	2	0	0	100	l		15			75				8	skeletal ooid grainstone
07H	3459.14	72	1.6	6.4	0	0	100	l		10			80				8	skeletal ooid grainstone
08H	3459.45	93	0	0	0	0	100	l	10			20					5	peloid skeletal wackestone
09H	3459.72	83.3	0	1.7	0	0	100	l		40			25				8	ooid skeletal grainstone
03V	3459.89	100	0	0	0	0	100	l	10				75				8	skeletal ooid grainstone

Plug No.	Depth (m)	Porosity (%)							Routin			Sedimentary Environments
		Interparticle	Intraclastic	moldic	intra-crystalline	vuggy	Fracture	Porosity	Permeability (mD)	Grain Density (g/cc)		
01H	3457.25											lagoon
01V	3457.4											lagoon
02H	3457.5			5			5	6.654	0.605	2.78		lagoon
03H	3457.98			10			10	4.616	7.002	2.62		lagoon
04H	3458.13						0	3.037	0.032	2.74		lagoon
05H	3458.62						0	9.443	16.490	2.62		ooid shoal
06H	3458.84						0	5.917	0.399	2.83		shoal margin
02V	3458.94						0	8.748	0.014	2.70		lagoon
07H	3459.14		20				20	22.818	0.743	2.69		ooid shoal
08H	3459.45		2	5			7	7.394	1.223	2.42		lagoon
09H	3459.72	2	5	5	3		15	10.323	0.304	2.70		shoal margin
03V	3459.89						0					ooid shoal

Figure 1: A part of petrography studies for the core plugs of well.

Table 1: FRF and porosity measurements at the confining pressure (6200 psi) for core plugs.

No.	Core Depth (m)	Grain Density (g/mL)	Gas Permeability (mD)	Formation Resistivity FRF	Porosity by brine (v/v)
1	3460.50	2.71	1.87	173.02	0.19
2	3461.26	2.72	1.78	213.71	0.22
3	3464.43	2.74	0.06	355.11	0.09
4	3465.78	2.76	0.24	404.33	0.17
5	3469.82	2.88	0.39	657.81	0.05
6	3535.63	2.79	21.7	96.47	0.10
7	3536.16	2.74	19.2	50.56	0.15
8	3542.17	2.85	428	23.00	0.23
9	3542.64	2.86	241	18.26	0.25
10	3568.73	2.87	0.01	953.00	0.02
11	3569.87	2.88	7.93	65.74	0.13
12	3572.06	2.87	410	22.98	0.24
13	3575.11	2.75	0.35	230.76	0.11
14	3579.66	2.73	1.26	263.72	0.15
15	3581.13	2.69	0.01	596.40	0.16
16	3597.44	2.73	<0.01	187.37	0.11
17	3599.39	2.72	0.00	813.53	0.03
18	3601.76	2.71	<0.01	1842.63	0.00
19	3603.33	2.72	<0.01	1778.29	0.01
20	3625.27	2.88	2.71	510.74	0.04
21	3627.90	2.86	35.5	64.71	0.13
22	3634.95	2.88	<0.01	1068.85	0.04
23	3638.43	2.85	2.07	138.73	0.09
24	3645.49	2.87	0.72	59.44	0.14
25	3646.96	2.87	0.07	684.38	0.04
26	3654.25	2.85	24.4	20.30	0.22
27	3660.49	2.86	0.05	272.86	0.03
28	3685.37	2.86	30.1	465.51	0.07
29	3688.81	2.85	5.57	72.77	0.15
30	3690.37	2.84	8.21	42.80	0.19
31	3691.69	2.84	0.73	203.79	0.09
32	3695.40	2.88	0.48	167.26	0.17

Determination of Petrophysical Parameters Based on the Conventional Methods

Based on the Archie equation, log-log plots of FRF versus porosity (Figure 2) and FRI versus water saturation (Figure 3) were used to determine petrophysical parameters. It is worth mentioning that two data points were out of range and were, therefore, removed.

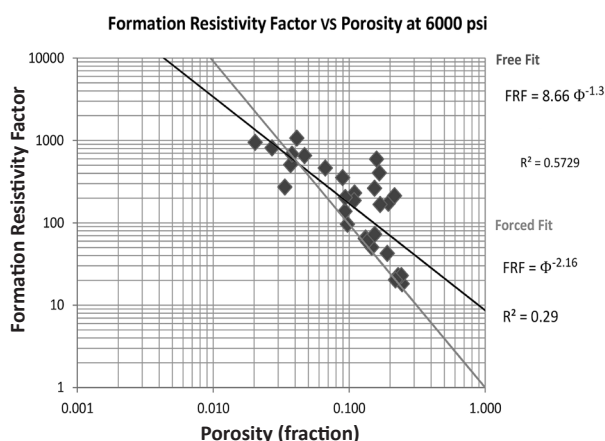


Figure 2: Determination of m based on log-log plot of FRF versus porosity using free and forced fit methods.

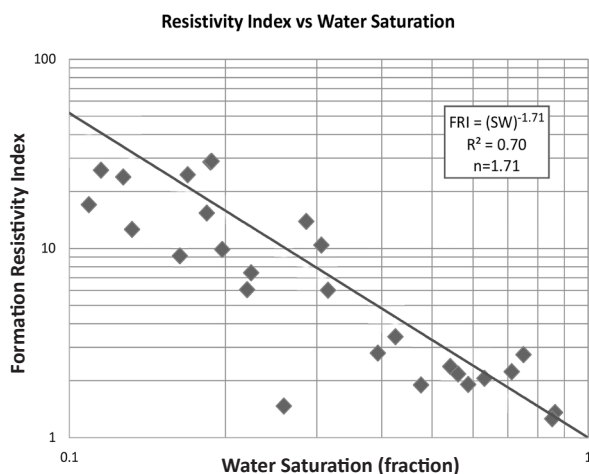


Figure 3: Determination of n based on the log-log plot of FRI versus water saturation.

According to Figure 2, in the forced fit method, the correlation coefficient of straight line ($R^2= 0.29$) is not good enough, so the obtained m is not acceptable. In addition, in the free fit method, the correlation coefficient ($R^2=0.57$) is not satisfying either, so the obtained m and a parameters will be uncertain.

An attempt was also made to determine m as a function of porosity (ϕ) and compare it with equations cited in the literature. Some of these commonly used equations are listed below:

- Borai established an equation for low porosity and tight carbonates as given below:
$$m=2.2-0.035 /(\phi+0.042)$$
- Shell recommended the equation below for evaluating low porosity carbonates:
$$m=1.87+0.019/\phi$$
- Sethi used the below equation:
$$m=2.05+\phi$$
- Rafiee et al. recommended a new equation for carbonate parts of the southwest Iranian oil fields as reads:
$$m=2.461-0.048/(\phi+0.031)$$
- Asadollahi et al. presented a relation between cementation factor and porosity in Iranian carbonate formations for both low and high porosity reservoirs as defined below [17-19]:
$$m=1 / (0.36-0.08 \ln(\phi))$$

Figure 4 illustrates the cementation factor values obtained by forced fitting method ($a=1$) versus porosity. The correlation coefficients (R^2) for both linear and power trend lines are not so suitable indicating that the m values belong to different rock types.

Figure 5 illustrates the graphs of Borai, Shell, Sethi, Asadollahi, and Rafiee relations, which show different trends with core data. Therefore, these formulas cannot be used for m values.

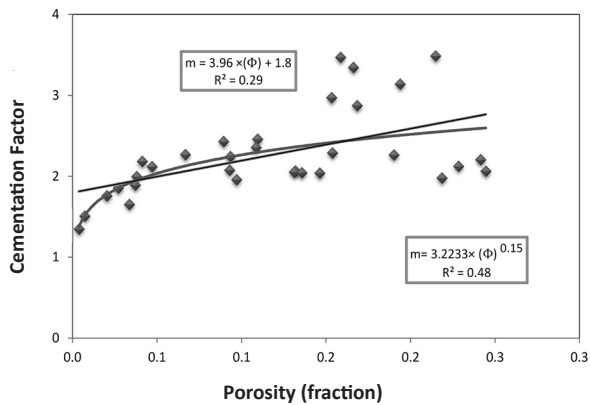


Figure 4: Relationship between cementation factor and porosity.

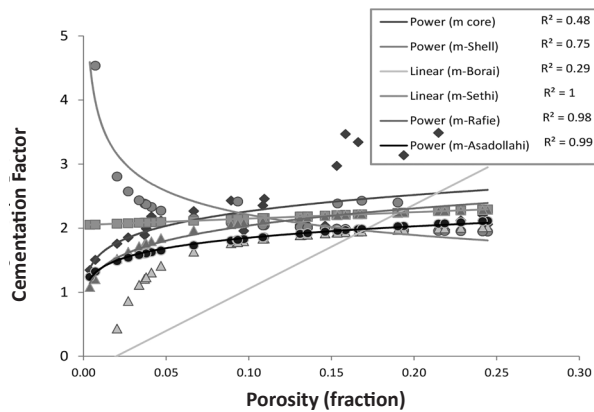


Figure 5: Cross plot of cementation factor versus porosity according to different empirical equations.

Determination of Petrophysical Parameters with Classifying Core Measurement Data Based on the Velocity Deviation Log (VDL)

The following equation is proposed to determine porosity from the transit time of compressional waves [20]:

$$\Delta T = (1 - \Phi) \Delta T_{ma} + \Delta T_f \quad (3)$$

where, ΔT_{ma} is the transit time for the unit length of the rock matrix, and ΔT_f is the transit time for the saturating fluid; Φ is the porosity.

Most often, for two porous media with identical porosities there might be velocities which do not conform to the Wyllie equation owing to the dissimilarities in the type of porosity. The velocity deviation log is referred to as the difference between the velocities obtained from the actual sonic log and that obtained from a synthetic velocity log by means of porosity log data in the time average equation. This method is proposed by Anselmetti and Eberli to

identify main porosity types in carbonate reservoirs. Generally, velocity is inversely proportional to porosity; however, the porosity types can potentially alter this relationship. In carbonate reservoirs, elastic properties are mostly governed by pore geometry [21, 22].

Anselmetti and Eberli studied the velocity deviation for five different types of porosity class corresponding to various samples to investigate the effect of pore geometry on velocity. They reported velocity deviations from positive to negative for various pore types, including intrafossil, moldic, interparticle, intercrystalline, and high micro-porosity. Pores with a low degree of connectivity within a densely cemented matrix usually give a positive deviation which corresponds to low permeability zones. For negative deviations, Anselmetti and Eberli indicated some factors other than lithology such as caving, borehole irregularities, and high content of free gas and/or fracture porosity [23].

According to the above explanations, velocity deviation logs can be obtained by the following equation:

$$VDL = V_{sonic} - V_{synthetic} \quad (4)$$

where, VDL is the velocity deviation log; V_{sonic} represents the velocity from sonic log, and $V_{synthetic}$ is the velocity calculated from one of the neutron, density, neutron-density logs, or core-plug porosity by using the Wyllie time average equation. Upon work done by Kazemzadeh et al., deviation logs derived from neutron-porosity logs showed better results for the determination of different pore types and petrofacies. In this study, the comparisons between different porosity logs also showed the same results. Therefore, neutron porosity log was used to obtain deviation velocity log [24]. Firstly, the environmental corrections were carried out on neutron-porosity log, and then, according to SGR log, it was corrected in terms of shale effect. Since the selected well had been drilled by water base mud, ΔT_f was considered 189.5 μ s/ft. Having lithology log and transit time data for each mineral, ΔT_{ma} log was obtained by using Apparent Matrix Properties module in Geolog (version 7) software.

Considering the following relationships, real and synthetic velocity logs were calculated to obtain VDL log.

$$V_{sonic} = 304.8 / \Delta T_{sonic} \quad (5)$$

$$V_{synthetic} = 304.8 / \Delta T_{synthetic} \quad (6)$$

According to the obtained VDL log, as it is shown in Table 2, the values of velocity deviation log for all the cores samples were high and could not be classified with respect to pore types. Analyzing core petrography results, it was recognized that, in many of the samples, anhydrate (with

a grain density higher than both dolomite and limestone) has filled pores in the form of patchy anhydrate cement, so it has increased real velocity and VDL.

Therefore, for these samples and those that have only moldic pore type, VDL will be high, and they cannot be classified in different groups. We can conclude that in situations like this VDL method will not be applicable to classifying core samples with respect to their pore types.

Table 2: VDL data based on shale corrected neutron porosity log at the core samples depth.

No.	Core Depth(m) (wire log depth matched)	VDL	Rock Category Code
			-500 <VDL<+500 : 1, +500 <VDL : 2, VDL<-500 : 3
1	3460.50	1021	2
2	3461.26	2718	2
3	3464.43	1310	2
4	3465.78	1751	2
5	3469.82	-1659	3
6	3535.63	4584	2
7	3536.16	2009	2
8	3542.17	2249	2
9	3542.64	2605	2
10	3568.73	1546	2
11	3569.87	1751	2
12	3572.06	1108	2
13	3575.11	2148	2
14	3579.66	2686	2
15	3581.13	1744	2
16	3597.44	1349	2
17	3599.39	1757	2
18	3601.76	577	2
19	3603.33	516	2
20	3625.27	2786	2
21	3627.90	3063	2
22	3634.95	2977	2
23	3638.43	3010	2
24	3645.49	1984	2
25	3646.96	2613	2
26	3654.25	2282	2
27	3660.49	2090	2
28	3685.37	2359	2
29	3688.81	3444	2
30	3690.37	3509	2
31	3691.69	2322	2
32	3695.40	3598	2

Determination of Petrophysical Parameters with Classifying Core Measurement Data Based on the Integration of Petrography and VDL Results

Knowing pore types and the geological description of the core samples based on the petrography data and considering VDL results, the core samples were classified in three groups as shown in Table 3. For each group, the log-log plots of FRF versus porosity are used for the determination of m in the forced fit, and FRI versus water saturation is employed to determine n (Figures 6-11).

Table 3: Classifying core samples according to pore types and geological description.

Rock Category	Geology Description	Data Frequency
1	Moldic pore type, without anhydrate	7
2	Interparticle and intercrystalline pore type, patchy anhydrate cement	15
3	Interparticle and Intercrystalline pore type, without anhydrate	10

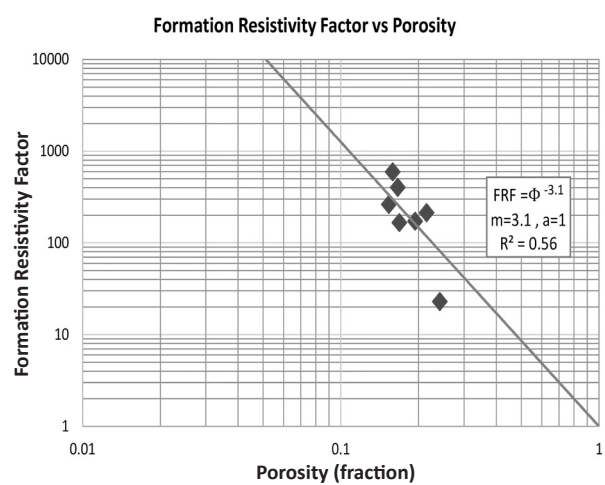


Figure 6: Relationship between FRF and porosity for rock category 1.

Table 4 summarizes the results of this classifying. As it is seen, the correlation coefficients (R^2) for all three groups (especially for group 2) are acceptable for the saturation parameters obtained.

Table 4: Summarized results of the determined petrophysical parameters for each category.

Category	a	m	R^2	n	R^2
1	1	3.1	0.56	1.93	0.62
2	1	2.18	0.90	1.57	0.90
3	1	1.67	0.73	2.27	0.67

In order to employ these petrophysical parameters as a continuous well log, it was required to obtain secondary (moldic) porosity log generated from the difference between neutron porosity log (total porosity) and sonic log (primary porosity). Therefore, based on the above explained classification, providing lithology and secondary porosity logs, the petrophysical parameters were obtained as a well log, and they were then applied to water saturation equations in petrophysical modeling (performed using Geolog commercial software).

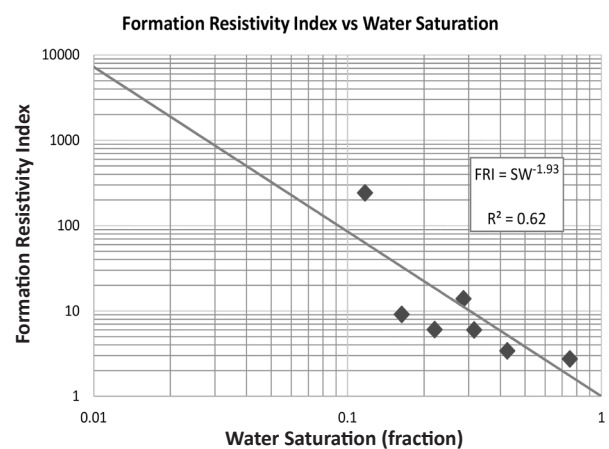


Figure 7: Relationship between FRI and water saturation for rock category 1.

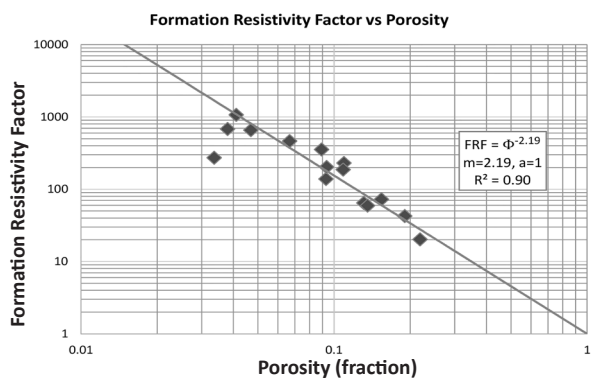


Figure 8: Relationship between FRF and porosity for rock category 2.

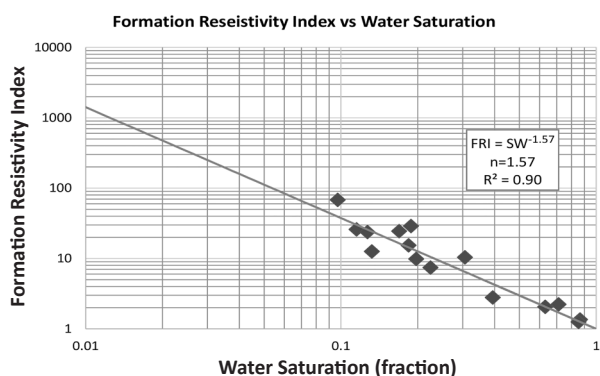


Figure 9: Relationship between FRI and water saturation for rock category 2.

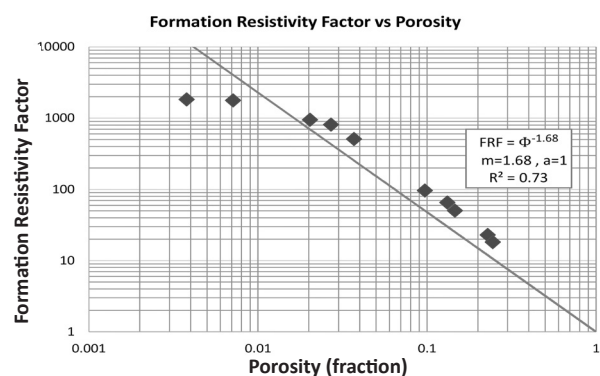


Figure 10: Relationship between FRF and porosity for rock category 3.

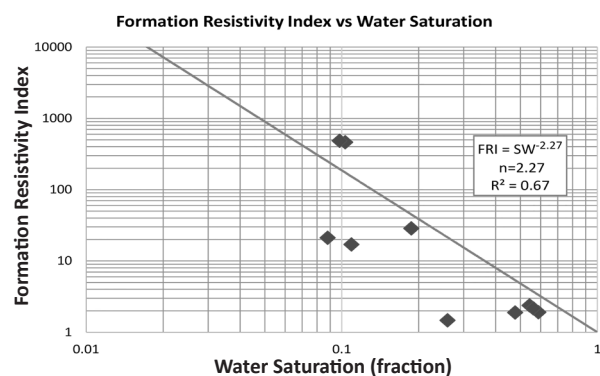


Figure 11: Relationship between FRI and water saturation for rock category 3.

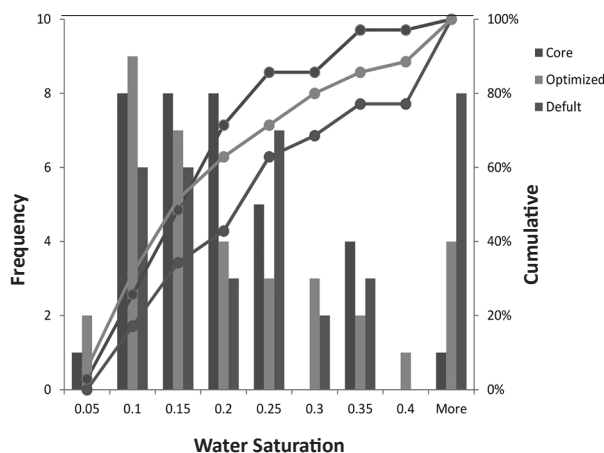


Figure 12: Cumulative histogram of the core and computed water saturation data.

Petrophysical Modeling and Analysis

As it was mentioned earlier, Geolog software, as a petrophysical analysis tool, was employed in this study to obtain water saturation log. To resolve a petrophysical problem, two different approaches are available. The first method is a deterministic method which is generally suitable for simple lithology problems. In this approach, porosity, shale fraction, and shale volumes (saturation) are computed sequentially. The second method is a multi-mineral approach referred to as Multimin. This approach is applied to complex lithology, where the minerals and rock pore fluids all affect the log responses. In this method, both log measurements and log response parameters are used in the log response equations, which will be solved simultaneously to compute the fraction volumes of formation minerals and fluids. Indonesia and other equations were selected here to compute fluid volumes and thus water saturation. Figure 13 shows a layout of Multimin analysis results for the candidate well. The log tracks on the right are water saturation logs computed based on the Indonesia water saturation equation.

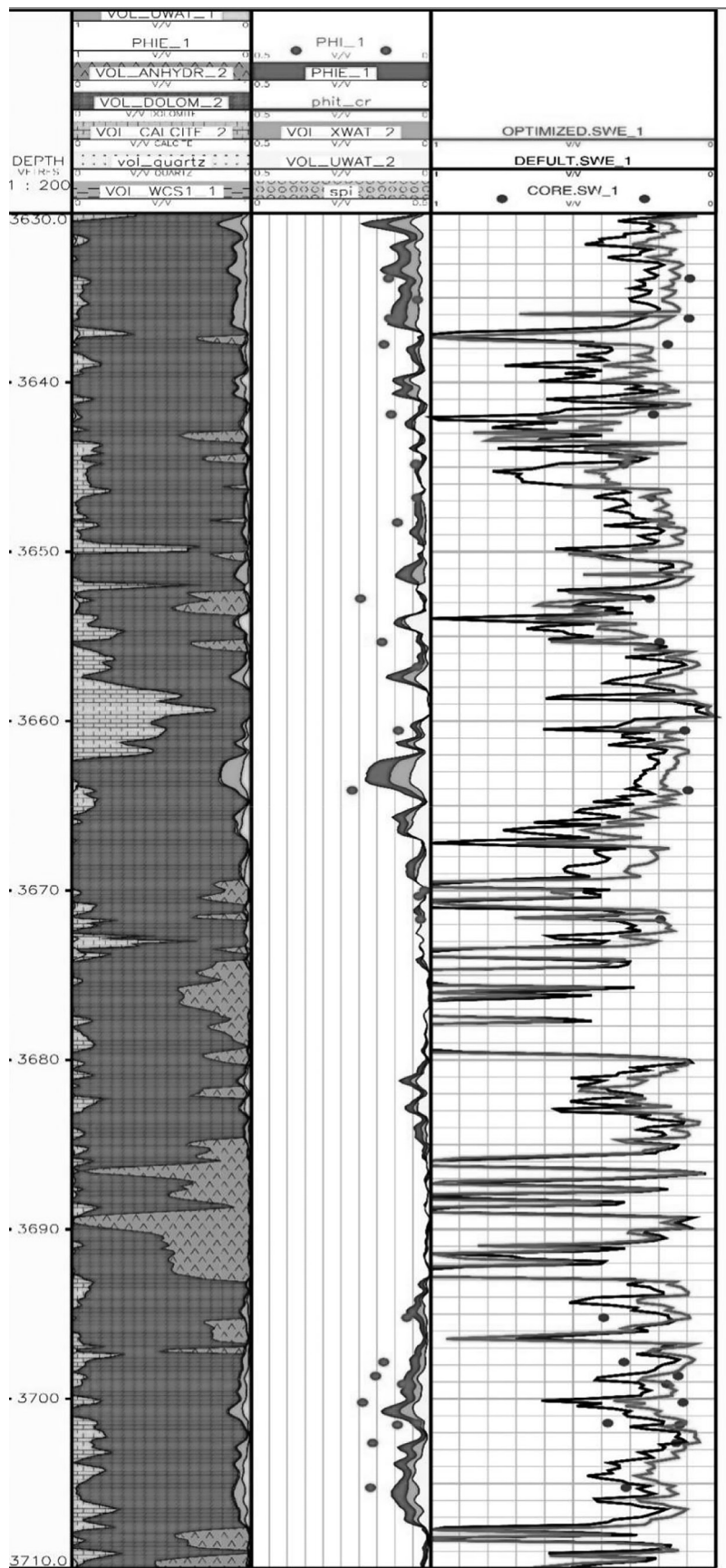


Figure 13: Computed water saturation (black and pink curves in the right track based on the default and the optimized petrophysical parameters) compared to the core data (blue dots).

The black curve refers to the water saturation computed based on default values ($m=2$, $n=2$, $a=1$), and the pink curve addresses the calculated water saturation based on the optimized parameters. Considering an average value of n instead of applying n as a variable resulted in a better match with the core data.

Several runs were performed according to different water saturation equations and different combinations of petrophysical parameters (i.e. as constant and/or variable values). Because of very low clay content in some parts of the reservoir, employing different water saturation equations did not make significant difference between the obtained water saturation logs. Moreover, other combinations of petrophysical parameters did not result in a better match with the core data.

In order to evaluate the accuracy of the optimized water saturation based on the default and the optimized petrophysical parameters compared to the core data, three error measures, including average error, standard deviation, and root mean square error (RMS) were used. The results of the error analysis are given in Table 5.

Table 5: Error analysis of the computed water saturation results based on the default and the optimized Archie's parameters.

Petrophysical Parameters	Average Error	Standard Deviation	Root Mean Square (RMS)
Default ($m=2$, $n=2$, $a=1$)	0.14	0.15	0.18
Optimized ($a=1$, $m=$ variable, $n=$ average value)	0.08	0.09	0.10

It is important to note that the error parameters for the optimized water saturation have considerably decreased compared to their default values, so using the optimized parameters for water saturation determination is recommended.

According to the cumulative histogram of water saturation data shown in Figure 12, both the optimized and the default data follow the trend of the core data. In addition, the optimized data are in good agreement with the trend of the core water saturation.

CONCIUSIONS

1. A considerable degree of uncertainty is observed when the cementation factor is determined according to the traditional method of calculating the slope of the forced and free straight line fitting to the data points on a log-log plot of FRI versus water saturation.
2. The cementation factor values determined according to the conventional methods of free and forced straight line fitting on the log-log plot of formation resistivity factor (FRF) versus porosity were uncertain.
3. According to cross plot of cementation factor values and porosity, a reliable equation to present cementation factor as a function of porosity was not achieved. Also, the empirical equations did not provide a good match with the core data points, and even Shell equation trend was in contrary to the trend of the core data.
4. Applying VDL approach to classify the core measurement data based on pore types is not applicable in cases that anhydrate exists in the core samples and fills pores as patchy cement.
5. Acceptable and reliable petrophysical parameters were determined by classifying the core measurement data based on core geological descriptions and VDL results.
6. The results of petrophysical modeling based on the multiminerall approach through Multimin module of Geolog software showed that applying m as variable and n as an average value in Indonesia water saturation equation would give a better

match between the calculated water saturation log and the core data points compared to applying other combinations of petrophysical parameters.

7. In petrophysical modeling, because of a very low clay volume in some parts of reservoirs, employing different water saturation equations did not make a significant difference between the calculated water saturation logs.
8. Error analysis and cumulative histogram showed that the water saturation data resulted in the optimized petrophysical parameters compared to the default ones, had a lower error, and were in good agreement with the trend of the core water saturation.

ACKNOWLEDGMENTS

The authors warmly thank the Research and Technology Department of Iranian Offshore Oil Company (IOOC) for supporting this work.

REFERENCES

1. Archie G. E., "The Electrical Resistivity Log as an Aid in Determining Some Reservoir Characteristics," *Transactions of AIME*, **1941**, 146, 54-62.
2. Worthington P. F., "The Evolution of Shaly-sand Concepts in Reservoir Evaluation," *The Log Analyst*, **1985**, 26, 23-40.
3. Hossin A., "Calcul des Saturations en Eau par la Methode du Ciment Argileux," *Bulletin de l'Association Francaise des Techniciens du Petrole*, **1940**
4. Simandoux P., "Mesures Dielectriques en Milieu Poreux, Application a la Mesure des Saturations en Eau," *Etude du Comportement des Massifs Argileux* Revue, IFP Supplementary Issue, **1963**.
5. Bardon C. and Pied B., "Formation Water Saturation in Shaly Sands," Trans. SPWLA 10th Annual Logging Symposium, **1969**.
6. Poupon A. and Leveaux J., "Evaluation of Water Saturation in Shaly Formations," SPWLA 12th Annual Logging Symposium, **1971**.
7. Waxman M. H. and Smiths L. J. M., "Electrical Conductivities in Oil-bearing Shaly Sands," *Society of Petroleum Engineers Journal*, **1968**, 8, 107-122.
8. Clavier C., Coates G., and Dumanoir J., "The Theoretical and Experimental Bases for the 'Dual Water' Model for the Interpretation of Shaly Sands," *Paper SPE 6859*, **1977**.
9. Aguilera R., "Analysis of Naturally Fractured Reservoirs from Conventional Well Logs," *Journal of Petroleum Technology*, **1976**, 28, 764-772.
10. Borai, A. M., "A New Correlation for the Cementation Factor in Low-porosity Carbonates," *SPE Formation Evaluation*, **1987**, 2, 495-499.
11. Lucia F. J., "Carbonate Reservoir Characterization," *Springer*, **1999**, 226.
12. Ragland D. A., "Trends in Cementation Exponents (m) for Carbonate Pore Systems," *Petrophysics*, **2002**, 43, 434-446.
13. Rezaee M. R., Motiei H., and Kazemzadeh E., "A New Method to Acquire m Exponent and Tortuosity Factor for Microscopically Heterogeneous Carbonates," *Journal of Petroleum Science and Engineering*, **2007**, 56(4), 241-251.
14. Towel G., "An Analysis of the Formation Resistivity Factor-porosity Relationship of Some Assumed Pore Geometries," in 3rd Annual Logging Symposium Transactions, SPWLA, **1962**.
15. Focke J. W. and Munn D., "Cementation Exponent in Middle Eastern Carbonate Reservoirs," *SPE Formation Evaluation*, **1987**, 155-167.
16. Hamada G. M., Almajed A. A., and Okasha T. M., "Uncertainty Analysis of Archie's Parameters Determination Techniques in Carbonate Reservoirs," *Journal of Petroleum Exploration and Production Technology*, **2013**, 3, 1-10.
17. Sethi D. K., "Some Considerations about the Formation Resistivity Factor-porosity Relations," 20th SPWLA Symposium, **1979**.
18. Rafiee S., Hashemi A., and Shahi M., "A New Cementation Factor Correlation in Carbonate Parts of Southwest Iranian Oil Fields," *Electronic Scientific Journal Oil and Gas Business*, **2013**, 2, 227-251
19. Asadollah M., Keramati M., Bagheri A. M., and Haghghi M., "Investigation of the Effect of Cementation Factor on OOIP in an Iranian Carbonate Reservoir," *GEO 2006 Middle East Conference and Exhibition*, **2006**.
20. Wyllie M. R. J. and Gregory A. R., "Formation Factors of Unconsolidated Porous Media: Influence of Particle Shape and Effect of Cementation," *Journal of Petroleum Technology*,

1953, 5, 103–110.

21. Anselmetti F. S. and Eberli G. P., "The Velocity-deviation Log: a Tool to Predict Pore Type and Permeability Trends in Carbonate Drill Holes from Sonic and Porosity or Density Logs," *AAPG Bull*, **1999**, 83, 450–66.
22. Brie A, Johnson D. L. and Nurmi R. D., "Effect of Spherical Pores on Sonic and Resistivity Measurements," Society of Professional Well Log Analysts 26th Ann. Logging Symp, **1985**
23. Eberli G. P., Anselmetti F. S., and Incze M. L., "Factors Controlling Elastic Properties in Carbonate Sediments and Rocks," *The Leading Edge*, **2003**, 22, 654–60
24. Kazemzadeh E., Nabi-Bidhendi M., Keramati Moezabad M., Rezaee M. R. and Saadat K., "A New Approach for the Determination of Cementation Exponent in Different Petrofacies with Velocity Deviation Logs and Petrographical Studies in the Carbonate Asmari Formation," *Journal of Geophysics and Engineering*, **2007**, 4, 160-170.